## Supplementary Material

Experimental details

The electrolyte solution comprised 1 M $LiPF_6$ in 3:7 EC:EMC v/v (premixed, soulbrain MI PuriEL R&D 280). Salts used to mimic dissolved transition metals were $Mn(TFSI)_2$ (Solvionic, 99.5%), $Co(TFSI)_2$ (Alfa Aesar, ≥95.0%), $Ni(TFSI)_2$ (Alfa Aesar, ≥97%), and $Cu(TFSI)_2$ (Sigma-Aldrich, purchased as the hydrate), all dried under vacuum at 100 °C. NEt_4BF_4 (Fluka Analytical, ≥99.0%) was added to some electrolyte samples. NMR spectra were collected on a Bruker Avance III HD 500 MHz spectrometer using a BBO probe, and sealed capillaries of C_6D_6 were added to NMR tubes for field locking and shift referencing. Solutions were prepared in an argon glovebox and NMR tubes were sealed with J-Young valves. The method of determining BMS shifts by comparing diamagnetic and paramagnetic samples is illustrated in Figure S1. Mn and Ni dissolution from $LiMn_2O_4$ (MTI), $LiNiO_2$ (Aldrich), and $LiNi_{0.5}Mn_{1.5}O_4$ (Aldrich) was assessed by storing 1.5 g cathode powder, 3 mL electrolyte solution, and 3 μL water in sealed aluminium vials at 60 °C for 20 days. Solutions were centrifuged to recover the electrolyte solution. Due to extreme dissolution, $LiNiO_2$ and $LiNi_{0.5}Mn_{1.5}O_4$ samples were diluted 25× and 100× with pristine electrolyte, respectively, before NMR measurement. ICP-OES samples were prepared in duplicate by dilution with nitric acid (trace metal grade); measurements were performed using an iCAP 7400 Duo ICP-OES Analyzer (Thermo Fisher Scientific).
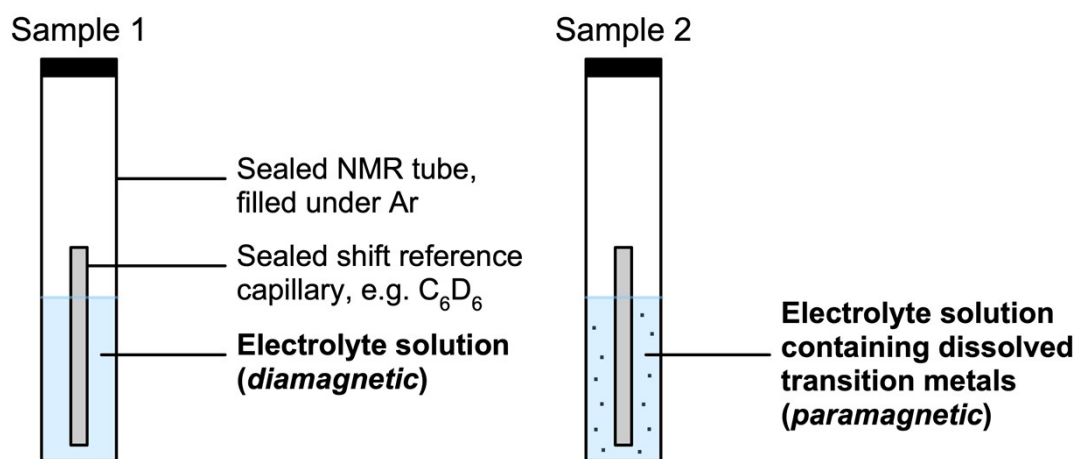
Figure S1. Diagram demonstrating the use of a solvent capillary in an NMR tube to determine the BMS shift. The BMS shift was extracted by comparing the chemical shift of a diamagnetic sample (Sample 1, referenced to the solvent capillary shift) to the chemical shift of a paramagnetic sample (Sample 2, also referenced to the solvent capillary shift).

BMS calibration fits

The χ_M values for dissolved Mn(TFSI)$_2$ and Ni(TFSI)$_2$ were used in Figures 2, 4, and S2 to calculate 'predicted' values of magnetic susceptibility and concentration (via Equation 1). Table S1 lists these extracted χ_M values, which were determined by applying a line of best fit through the calibration points of the susceptibility vs concentration plot in Figure 1f–i and forcing a *y*-intercept of 0 (i.e., the equation of the line is $y = \chi_M{\cdot}x$). The coefficient of determination values (R^2) for the lines of best fit are also provided.

Table S1. Mn^{2+} and Ni^{2+} molar magnetic susceptibilities, as determined from linear fits of Figure 1f–i (magnetic susceptibility from ^{1}H BMS shift vs metal concentration), and the R^2 values for those fits.

|		EC (Figure 1f)	EMC ethyl CH$_2$ (Figure 1g)	EMC methyl (Figure 1h)	EMC ethyl CH$_3$ (Figure 1i)
Mn^{2+}	χ_M (mL· mol^{-1})	0.0165	0.0158	0.0158	0.0154
	R^2	0.9994	0.9996	0.9996	0.9996
Ni^{2+}	χ_M (mL· mol^{-1})	0.00493	0.00460	0.00459	0.00456
	R^2	0.9990	0.9981	0.9981	0.9986

Magnetic moments

Table S2 lists the μ_{eff} values determined for dissolved Mn(TFSI)$_2$, Ni(TFSI)$_2$, Co(TFSI)$_2$, and Cu(TFSI)$_2$. μ_{eff} values were calculated using Equations 1–2 after measuring the EMC ethyl CH$_3$ BMS shift in a 5 mM solution of paramagnetic ions.

Table S2. Effective magnetic moments of dissolved Mn^{2+}, Ni^{2+}, Co^{2+}, and Cu^{2+}.

	μ_{eff} (μ_{B})
Mn^{2+}	6.07
Ni^{2+}	3.28
Co^{2+}	5.14
Cu^{2+}	2.12

LiMn$_2$O$_4$ storage in non-acidified electrolyte

To study Mn leaching in a non-acidified electrolyte solution (i.e., where HF was not formed via the addition of water to the sample), 3 g LiMn$_2$O$_4$ was stored with 7 mL electrolyte solution and in an aluminium bottle at 60 °C for 77 days. The procedure to isolate the electrolyte solution and measure the BMS shift is the same as described in the main text, and results are shown in Figure S2.
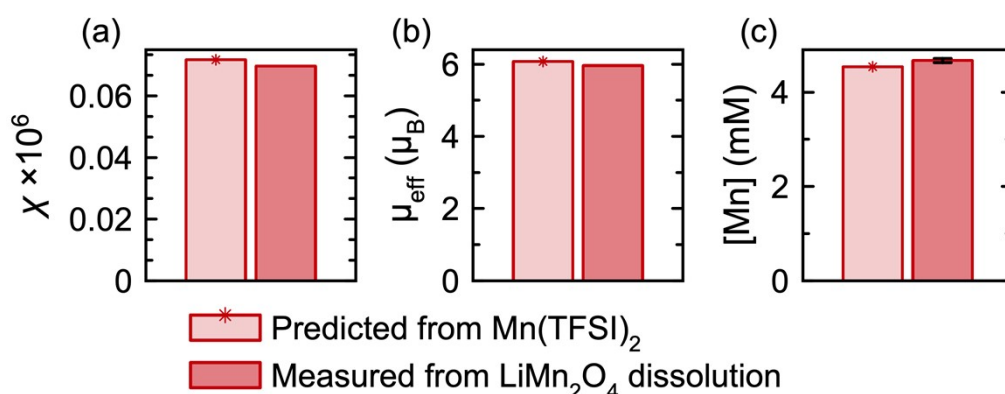
Figure S2. (a) χ, (b) μ_{eff}, and (c) concentration for Mn dissolved from LiMn$_2$O$_4$. Predicted χ arises from the Mn(TFSI)$_2$ χ_M (from the correlation in Figure 1i) multiplied by the ICP-OES concentration; predicted μ_{eff} is that reported in Figure 3 for Mn(TFSI)$_2$; and predicted Mn concentration arises from the sample χ divided by the Mn(TFSI)$_2$ χ_M. Error bar in panel (c) indicates the standard deviation of three ICP-OES samples.

The close match between Mn(TFSI)$_2$ predictions and sample measurements (Figure S2a and S2b) shows that Mn dissolved from LiMn$_2$O$_4$ in non-acidified electrolyte solution exists exclusively as Mn^{2+}. If quantification is of interest, a good estimate of Mn concentration is achieved by NMR as compared to the ICP-OES value (Figure S2c) by assuming that all Mn is Mn^{2+} and applying the Mn(TFSI)$_2$ χ_M. The BMS shift predicts 4.54 mM Mn^{2+}, and ICP-OES showed 4.67 ± 0.05 mM Mn.

ICP-OES of LiNi$_{0.5}$Mn$_{1.5}$O$_4$ sample

Metal concentrations in the LiNi$_{0.5}$Mn$_{1.5}$O$_4$ sample were not predicted by NMR, as many possible combinations of Ni^{2+} and Mn^{2+} may yield the same BMS shift. ICP-OES results showed that the NMR sample contained 2.982 ± 0.006 mM Mn and 2.84 ± 0.05 mM Ni.